Band Offset Models of 3D-Bonded Semiconductors and Insulators

Y Guo[1,2*], H Li[1], S J Clark[3], J Robertson[1],

1 Engineering Dept, Cambridge University, Cambridge CB3 0FA, UK
2 School of Engineering, Swansea University, Swansea SA2 8PP, UK
3 Physics Dept, Durham University, Durham DH1 3LE, UK
* yuzheng.guo@swansea.ac.uk

Abstract The band offsets of heterojunctions of three-dimensionally (3D) bonded semiconductors lie between two limits, the electron affinity rule (unpinned limit) and the matching of the charge neutrality levels (CNLs), equivalent to the pinned limit. It is shown that it has been difficult to compare the validity of these cases because most experimental and theoretical tests require a lattice-matching across the heterojunction, and most semiconductors with the same lattice constant have similar average band energies referred to the vacuum level. A second point is that the CNL when referenced to the vacuum level varies surprisingly weakly with the midgap energy with respect to the vacuum level. A calculation of band offsets for heterojunctions with larger lattice mismatch provides a stronger test, and this result is found to favour the CNL matching model. This result is important for many practical device heterojunctions, where unmatched interfaces are common.

Introduction

Most semiconductor devices require knowledge of the band alignment at the interfaces within them, whether these are between two semiconductors, between a semiconductor and an insulator, or the Schottky barrier interface between a metal electrode and a semiconductor. For many years, the only inorganic semiconductor interfaces that could be modelled were the epitaxial heterojunctions, such those in quantum well lasers or high electron mobility transistors (HEMTs). Nowadays, there is an expectation to model more complex systems, such as solar cells, light emitting diodes, catalytic systems, or chemical sensors, which might be poly-crystalline, multilayered or with functionalised surfaces. This leads to a desire for more general models of band offsets.

The band offsets can be found by density functional calculations on supercell models of the heterojunctions.[1-10] This is aided if the two components are well lattice-matched, otherwise this requires large supercell periodicities along the interface to ensure commensurate lattices, or interfaces with mismatch defects like dangling bonds. Thus, there is also a desire for simplifying principles able to predict band offsets under more general situations of poor lattice-matching.

In broad terms, there are two limiting cases for the band offset.[1-11] The first ‘natural’ band offset where there is no charge transfer across an interface and so the conduction band offset is simply the difference between the electron affinities of the two semiconductors, as in the electron affinity model.[1-3] The second case is where there is significant charge transfer across the interface, so that the ‘bare’ band offset is screened by the charge transfer across the interface.[4-6] This case applies to interfaces between the inorganic 3-dimensionally bonded semiconductors. To these limits can be added the effects of any dipole layers.

These two limits are related respectively to the unpinned (Schottky) and pinned (Bardeen) limits of Schottky barriers.[11-13] Interestingly, while the behaviour of the Schottky barriers of a particular semiconductor is reasonably well settled, the situation is less well settled for their heterojunctions, and it often results in the default use of the electron affinity model[14] Here, we study why this has been so. To do this, we investigate some specific semiconductor pairs with more extreme differences than usual, such as larger lattice mismatches. The results of this favor the pinned limit. We cover four broad classes of materials, the 3-dimensionally bonded semiconductors like Si and GaAs, the insulators like HfO_2, the transparent conductors like SnO_2 and the 2D semiconductors like MoS_2. Once these questions are settled, we can extend their use to more complex systems. In order to test the band offset models, we need accurate values for the band gaps, and electron affinities, and reference levels.[15-16] We use hybrid functionals to correct the band gap error of the semi-local forms of density functional theory (DFT).

It should be noted that our analysis applies to 3D bonded semiconductors and insulators, and to the limited case of 2D layered systems like MoS_2 with vand der Waals inter-layer bonds. On the other hand, molecular semiconductor systems involve many additional phenomena that set their band alignments which tend to follow different set of rules which can be dominated by for example dipole alignment effects.[17-20]

Methods

The band gap, electron affinity (EA), and ionization potential (IP) of each semiconductor system are calculated here using a supercell model consisting of a slab of 8 layers of semiconductor and a 20Å of vacuum layer. The semiconductor slab is terminated by a non-polar surface. The electrostatic potential in the vacuum region is used to define the vacuum level energy. For the direct calculations of band offsets, we use supercells containing 6 layers of each semiconductor joined by their non-polar surfaces, both with and without a vacuum layer.

The calculations are carried out using the plane wave pseudopotential code CASTEP.[21] The atomic geometries are relaxed within the PBE version of the generalised gradient approximation (GGA). In this case, ultrasoft pseudopotentials are used with a plane wave cutoff of 400 eV, which converges the total energy to within 0.01 eV per atom. A 5x5x1 MP k-point mesh is used for geometry optimization. The residual force is less than 0.02eV/Å. A 11x11x1 k-point mesh is used to calculate the density of states. For layered compounds, the Grimme[22] dispersion correction is used to correct the DFT error for the van der Waals interaction and the associated bond lengths. Spin-orbit coupling is not included.

For both 3D and layered compounds, the band gap error of the GGA is corrected by using hybrid functionals, such as the Heyd-Scuseria-Ernzerhof (HSE)[23] functional or screened exchange (sX) hybrid functional.[24] In the latter case, norm-conserving pseudopotentials were used with an energy cutoff of 750 eV.

The HSE and SX functionals mix a certain fraction of screened Hartree-Fock (HF) exchange into the DFT exchange-correlation functional[23,24]. The calculated band gap for various compounds is given by Chen et al[15,16] and Hinuma et al[8] for HSE and by Clark and Robertson[24] for SX. The SX band gaps match the experimental values well over a wide range of band gaps. On the other hand, the HSE band gaps match well for a smaller range of gaps but then they decline for larger gaps. Recently, it has become common to adjust the band gap by varying the fraction of exact exchange mixed into the exchange-correlation functional. One way would be to

ensure the linearity of the total energy with fractional occupation across the band gap.[25] Another way is vary the fraction of exchange used in proportion to the inverse optical dielectric constant.[26,27,16]

Results

A Band Gaps and Electron Affinities

Table 1 compares the calculated band gaps and electron affinities of the various tetrahedrally bonded semiconductors calculated with the SX functional. These are compared to their experimental values from the compilation of Brillson.[28] Fig. 1 compares the calculated GGA and SX band gaps against the experimental band gap values.

Fig. 2 shows the variation of the GGA and SX values of electron affinity and ionisation potentials for the various semiconductors. We see that the SX values are wider than the GGA values for both valence and conduction bands.

Chen et al[15] have checked the alignment of hybrid functional band energies with those of GGA and with each other using the calculated electrostatic potential of the bulk semiconductors as a reference. In the case of SX, we used the band edge energies with respect to the potential in the vacuum gap to align the GGA and SX band energies, which is equivalent to using the vacuum potential as the reference level.

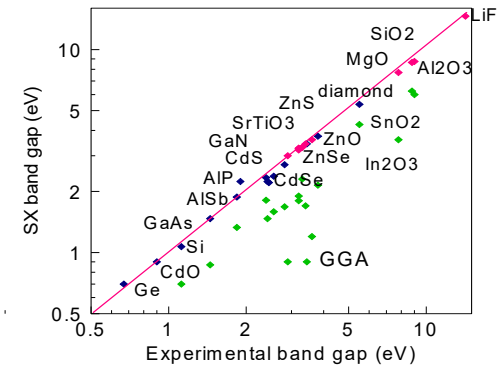

Fig. 1. Variation of calculated band gap with experimental gap, showing calculated GGA (green) and SX (red, blue) gaps.[24]

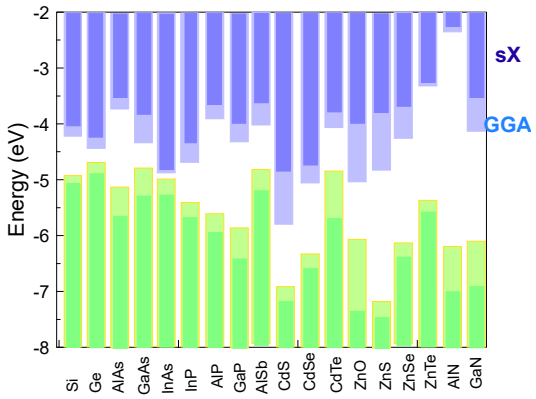

Fig. 2. The calculated electron affinity and ionisation potentials for tetrahedral semi-conductors, in the GGA and SX functionals.

Table 1. Calculated SX values of band gap, electron affinity (EA), ionization potential (IP), charge neutrality level above VBM, and their experimental values, for 8-electron semiconductors.

eV	Gap, SX	EA, SX	IP, SX	CNL	Gap, exp	EA, exp
Si	1.10	-4.00	-5.10	0.20	1.11	-4.05
Ge	0.67	-4.20	-4.87	0.10	0.67	-4.00
AlAs	2.17	-3.50	-5.67	0.85	2.16	-3.50
GaAs	1.50	-3.80	-5.30	0.50	1.43	-4.07
InAs	0.50	-4.80	-5.30	0.45	0.36	-4.90
InP	1.35	-4.35	-5.70	0.93	1.35	-4.35
GaP	2.29	-3.65	-5.94	0.83	2.26	-3.65
AlP	2.46	-3.97	-6.43	1.30	2.45	-3.98
AlSb	1.62	-3.60	-5.22	0.53	1.60	-3.60
CdS	2.41	-4.79	-7.20	1.90	2.42	-4.79
CdSe	1.88	-4.72	-6.60	1.50	1.73	-4.50
CdTe	1.64	-4.06	-5.70	1.12	1.58	-4.28
ZnO	3.43	-3.97	-7.40	3.27	3.39	-4.20
ZnS	3.74	-3.76	-7.50	1.75	3.60	-3.82
ZnSe	2.73	-3.67	-6.40	1.60	2.70	-4.09
ZnTe	2.36	-3.24	-5.60	1.09	2.25	-3.53
AlN	6.20	-0.80	-7.00	3.08	6.20	-0.60
GaN	3.39	-3.50	-6.89	2.14	3.20	-3.30

Table 2. Calculated SX values of band gap, electron affinity (EA), ionization potential (IP) and charge neutrality level above VBM for various oxides, and the experimental values of gap and EA.

eV	Gap, SX	EA, SX	IP, SX	CNL	Gap, exp	EA, exp
ZnO	3.40	-4.00	-7.40	3.27	3.40	-4.1
In_2O_3	2.70	-4.10	-7.00	3.30	2.60	-4.1
SnO_2	3.60	-4.80	-8.30	4.10	3.60	-4.8
TiO_2	3.20	-4.10	-6.30	2.20	3.20	-4.1
$SrTiO_3$	3.20	-4.10	-7.30	2.60	3.20	-4.1
$LaAlO_3$	5.60	-2.00	-7.60	3.80	5.60	-2
Cu_2O	2.10	-3.50	-5.60	0.80	2.10	-3.5
$CuAlO_2$	2.80	-1.90	-4.81	0.90	3.00	-1.9
$CuGaO_2$	2.30	-2.80	-5.10	0.80	2.40	-2.8
$CuInO_2$	2.00	-3.20	-5.20	0.80	2.00	-3.2
$CuCrO_2$	2.90	-2.70	-5.60	1.10	3.00	-2.7
$SrCu_2O_2$	3.30	-2.20	-5.50	2.00	3.00	-2.2
$ZnCo_2O_4$	2.36	-1.20	-3.60	2.40	2.30	-1.2
NiO	3.50	-1.10	-5.10	1.80	4.10	-1.1
$BiFeO_3$	2.85	-3.30	-6.15	1.90	2.80	-3.3
HfO_2	5.60	-2.20	-7.80	3.70	5.80	-2.2
La_2O_3	6.19	-1.90	-8.09	2.40	6.10	-1.9
Al_2O_3	8.64	-1.20	-9.84	5.50	8.80	-1.2
MgO	7.72	-0.80	-8.52	4.00	7.80	-0.8

SiO_2	8.75	-0.90	-9.65	4.50	9.00	-0.9

We also consider various functional oxides such as the transparent conducting oxides (TCOs) used in displays and solar cells, and the high K oxides used as gate dielectrics in CMOS. These systems can be a more extreme test of the calculations of band gap and band offsets. Table 2 gives the calculated band gaps, electron affinities and ionisation potentials of such oxides from SX and compares them to the experimental values from compilations of Hosono[29], Klein[30,31], Hattori[32], Greiner[33] and Robertson[34].

Fig 3 shows the calculated SX electron affinities and ionisation potentials for various oxides, both conducting and non-conducting. Fig. 4 compares the calculated ionisation potentials of some oxides with their experimental values. Whereas the GGA band gap is typically a 30% under-estimate for semiconductors, there can be a much larger error of up to 75% for the TCOs.

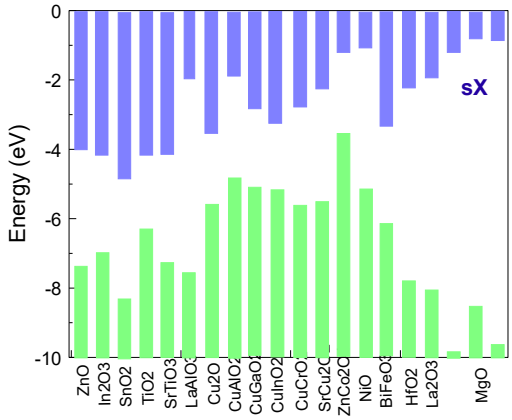

Fig. 3. Calculated electron affinities and ionisation potentials for various oxides, using the SX functional[34].

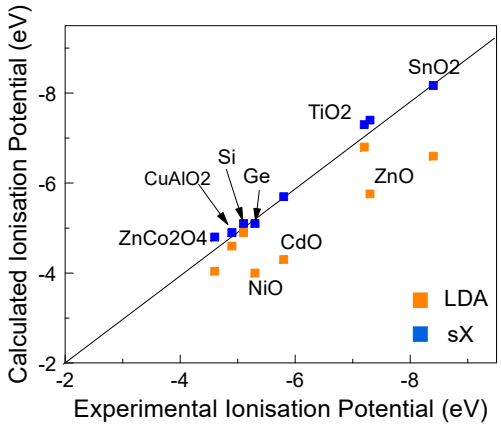

Fig. 4. Calculated GGA and SX values of ionisation potential vs. their experimental values[29-34] for some oxides.

For many technologically important systems like the TCOs, the band gap error can be particularly large and it arises from two separate effects. The first is the direct, semi-local DFT

under-estimation of the valence – conduction band gap, while the second is the effect of the semi-core levels of the cations[18]. This occurs for post-transition metal cations such as Zn, Cd and In. Here the upper valence states consist of anion p states and these are repelled upwards by the cation semi-core states[18,35]. Self-interaction causes the semi-core states to be too high in GGA, and they have repelled the valence band maximum (VBM) upwards which now lies too high. The hybrid functionals will move the core states down in energy and so lessen the upward repulsion of the VBM state. This effect occurs in the n-type TCO compounds like ZnO, and in the solar cell compounds like $CuInSe_2$.[34-37]

As an example, Fig. 5 shows the development of the electron affinities and ionisation potentials of ZnO from GGA to HSE to SX and compared to experiment. It is seen that HSE for the standard mixing fraction of $\alpha = 0.25$ has a gap of only 2.3 eV and it opens up considerably more on the CBM side when moving to SX. SX has improved the VB energy because it has moved the Zn 3d states down more.[38] The band gap of ZnO opens up as its HF screening parameter reduces, with the VBM and CBM moving away symmetrically from the gap center.

We see that our band energies are similar to those of Stevanovic et al[36]. On the other hand, there are differences to the well-known compilation of van der Walle and Neugebauer[39]. This is mainly because their band energies used the earlier, less accurate GGA+U method.

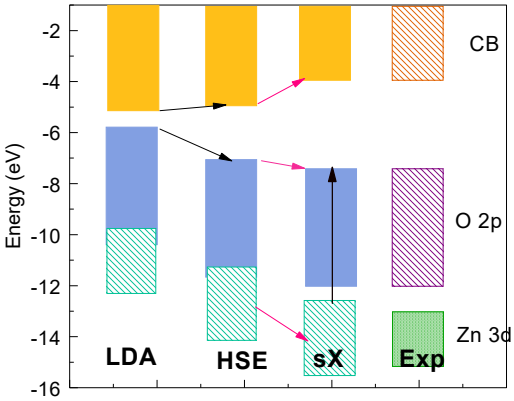

Fig. 5. Development of the valence band maximum, conduction band minimum and Zn 3d core levels, from LDA to HSE to SX, compared to experiment.

Many p-type TCOs are Cu oxide compounds.[40,41] The Cu 3d states lie at similar energies to the O 2p states, and their interaction lowers the effective mass of the O 2p states when they form the upper valence band. A number of p-type TCOs are from the defossalite family of hexagonal layer compounds.[42-44] Here we choose the (1101) faces as the nonpolar faces. The defossalites are notable for having the main optical absorption edge significantly above the minimum gap, due to low optical matrix elements for transitions to the lower conduction bands.

The high K oxides used as gate dielectrics are all closed-shell wide band-gap systems. The metals are very electropositive so the oxides have a high heat of formation, and the oxides cannot be reduced by reaction with Si. They include the oxides of Hf, Zr, La, Y, Sc, Lu, Sr, and Ba.[14,34,45] The rare-earth oxides such as Gd_2O_3 are also possible high K oxides[46], if their 4f states are out of the gap. On the other hand, TiO_2, $SrTiO_3$ and Ta_2O_5 do not have a sufficiently high heat of formation and will react with Si.[14] All these oxides have a roughly 30% band gap error.

$BiFeO_3$ is an interesting multiferroic oxide[47], where Fe is the magnetic ion, and Bi is the ferroelectric ion, where the distortion polarises its 6s lone pair state. $BiFeO_3$ has the R_{3c} crystal structure, and its antiferromagnetism is aligned along its z-axis. NiO is representative of another family of p-type oxides.[48] It is an open-shell oxide with a wide Ni 3d-like upper valence band. It has the rocksalt structure, and is antiferromagnetic along the (111) axis as in $BiFeO_3$.

Charge Neutrality Level

The vacuum level acts as a reference level in the electron affinity rule. In the charge transfer model, the reference level for the charge transfer across an interface is the charge neutrality level (CNL) of the semiconductor. The charge transfer across a semiconductor heterojunction depends on the evanescent states of the narrower gap side decaying into the gap on the larger gap side[4]. These evanescent states are the analogues of the metal induced gap states (MIGS) at the metal-semiconductor interface (Schottky barrier). The MIGS are intrinsic to the semiconductor side and represent a smearing of the surface states on a free semiconductor surface. The CNL is the energy at which the MIGS are filled up to for a neutral surface. They are also the branch point of the complex band structure in the gap.

The CNL can be calculated from the bulk electronic density of states N(E') from the zero of its Greens function[7,49-53,14],

$$G(E) = \int_{-\infty}^{\infty} \frac{N(E').dE'}{E - E'} = 0 \qquad (1)$$

The integral is taken over the Brillouin zone and the sum is over all bands.

A key question is how many valence or conduction bands should be included in the sum. In the original expression, the limits on the number of bands were infinite. The integral becomes convergent by including the wavefunctions in the integral, as was done in the original Tersoff formulation.[7] Originally, we used an atomic orbital basis set for the calculation of CNLs.[14] When using a plane wave basis set, we included only the same number of bands as in the tight-binding description[34,51], that is four valence bands and four conduction bands for a zincblende semiconductor, and the equivalent for other lattices or d-band compounds.[51] A similar counting was used by others.[49] In practice, the resulting CNL values for wide gap oxides were relatively insensitive to the choice.

However, this choice was less suitable for semiconductors with wider bands, where the convergence was poor. Schliefe et al[52,53] used fewer bands when calculating the CNLs of tetrahedral semiconductors, and this gave values slightly closer to those of other formulations.[54] The latter choice is supported if one inspects the imaginary band structure of various systems[55,56], where the branch point is taken from the imaginary bands closest to k=0. For HfO_2, a good choice is to include four bands[57], but for semiconductors, one band clearly lies much closer to k=0 than others.[55,56] Hence, for semiconductors we now include the same number of bands as in Schliefe et al[52,53].

Band Offsets

The heterojunctions of two semiconductors are constructed by joining them by a non-polar surface, such as (110) for zincblende structures. The band offsets are then given in the linear model as[14],

$$\Delta_n = (\chi_a - \Delta_{CNL,a}) - (\chi_b - \Delta_{CNL,b}) + S(\Delta_{CNL,a} - \Delta_{CNL,b}) \quad (2)$$

Here ϕ_n is the conduction band offset, χ_a is the electron affinity of *a*, $\Phi_{CNL,a}$ is the CNL of *a*, and S is the pinning factor, defined as $S = \partial\phi_n/\partial\Phi_M$, where Φ_M is the metal work function. Eqn (2) is an extension of the Cowley-Sze[58] model of Schottky barriers to heterojunctions.

The two limits of the electron affinity rule (S=1) and the CNL matching rule (S=0) can be regarded as using an external reference energy (the vacuum level) or an internal reference level of the semiconductor (the CNL/branch point of its bulk band structure). These points were noted earlier when Harrison[6] first proposed that band offsets should be referenced to the vacuum level, but then Harrison and Tersoff [9] over-ruled this model when realising that screened band offsets should be used. However, the numerical inaccuracies of their tight-binding approach prevented a full testing of their arguments.

Experimental[59,60] and theoretical supercell tests[10-12,61] of these two limits require lattice-matching of the two sides. To an extent, strain can be used to match the two components, and then the effect of the strain adjusted for in the energies with respect to the vacuum level. On the other hand, a more direct, significant test would involve two components whose band energies are likely to lead to significant charge transfer.

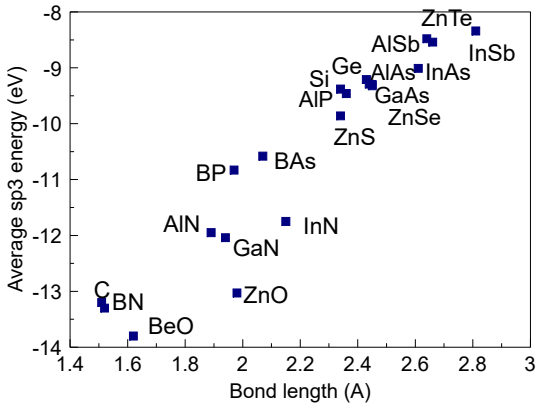

Fig. 6. The strong correlation between the sp^3 hybrid energy in tight-binding and bond length of the various tetrahedrally-bonded semiconductors

Fig. 6 shows the variation of the average sp^3 orbital energy (from the atomic orbital energies) vs. the bond lengths for the tetrahedrally bonded binary semiconductors. These show a close correlation between the average sp^3 energy and the bond length. Thus by requiring lattice matching, one chooses pairs of semiconductors with similar average sp^3 energy, and so they are unlikely to have a large charge transfer across their interfacial bonds, as Harrison and Tersoff[9] noted.

A second point concerns the CNL values that enter into CNL matching limit. Fig. 7(a) shows the variation of CNL energies referred to the vacuum level versus the average of the electron affinity and ionisation potentials (the midgap energy). The data are fitted by a line of slope S=0.34. This means that the CNL does not lie at a constant fraction of the band gap, but has a trend that if the average band gap energy moves down, away from the vacuum level, the CNL

energy moves upwards in the gap, to give much less overall shift than might be expected. A similar effect occurs in oxides[40] Fig.7(b), where the data is more scattered but has a similar trend.

Thus, a comparison of heterojunctions for the two limits using lattice-matched pairs[8,10,59] will not give as great a difference of band offsets as might be expected.

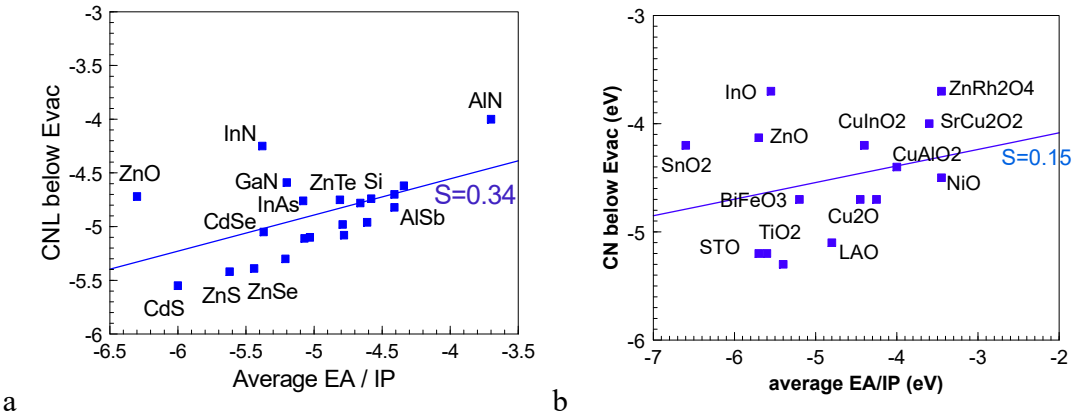

a b

Fig. 7. (a) The weak variation of the CNL energy (wrt. vacuum level) vs. the average of electron affinity and ionisation potential for (a) tetrahedral semiconductors. Slope = 0.34. (b) Variation for the various oxides. The slope of the line is 0.15.

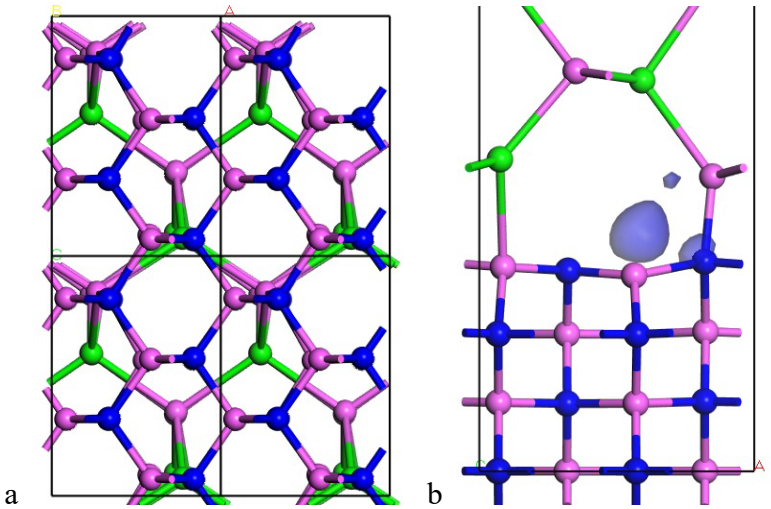

a b

Fig. 8. (a) Top and (b) side view of the zincblende (110)AlN:AlSb heterojunction with a √2:1 lattice-matching. Al= pink, N= blue, Sb=green. The blue shape in (b) is the dangling bond orbital at the unbonded interface N site.

To provide a more robust test of these two limits, we do not consider band offsets of lattice-matched pairs, but between pairs with a large mismatch of √2. The surface unit cell of (110) is √2 x 1, so that it is possible to match lattices of size ratio √2 in hypothetical heterojunctions if the second lattice is rotated by 90^0, as shown in Fig 8(a). The chosen pairs are AlSb or ZnTe for the larger lattice constant, and zincblende AlN, GaN and ZnO for the smaller lattice. Fig 8(b) shows

a side-view of bonding at these interfaces. The side-view shows that not all of the bonds continue across the interface, some dangling bonds (DBs) remain on the short lattice side.

There are two types of possible interface bonding for these mismatched cases. Fig 8(a,b) shows the case of interest here, with more polar semiconductors like AlN, GaN and ZnO on the short lattice side. Here a fraction of the sites on this side have no partners on the large lattice side, and these DBs undergo a charge transfer between each other which stabilises them, and causes their DB states to move outside of the band gap. The absence of gap states in this case of GaN is seen in Fig 9.

On the other hand, for an interface with a lesser mismatch, the interface sites are generally able to satisfy their bonding requirements by forming some like-atom (homopolar) bonds across the interface, in addition to heteropolar bonds. This case is unsuitable for our purpose because it can lead interface gap states which complicate the band alignment question.

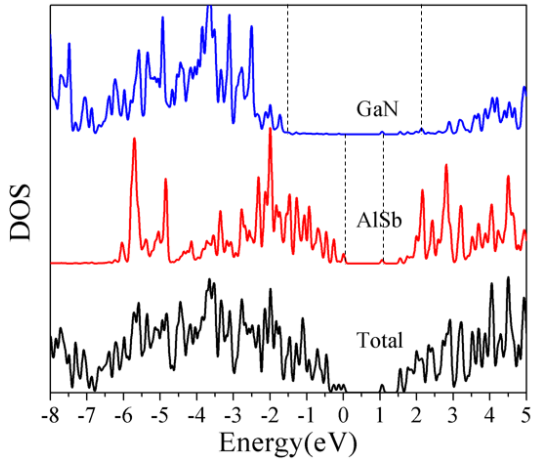

Fig. 9. Partial density of states in SX for GaN and AlSb layers at the (110)GaN:AlSb heterojunction. Note the absence of gap states for GaN. Vertical lines denote band edges.

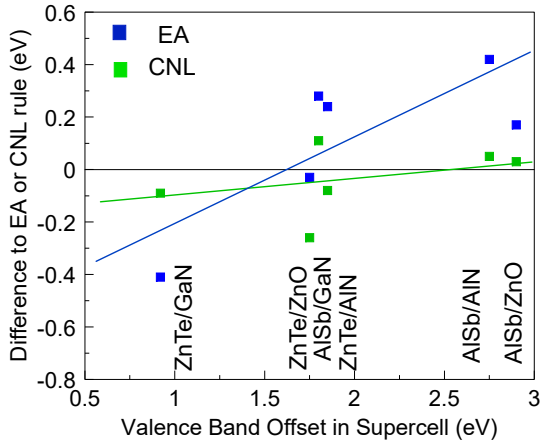

Fig. 10. Deviation of the calculated VB offsets for supercell models and VBO values estimated using the EA rule (blue) and the CNL matching rule (green).

We consider a supercell consisting of 6 layers of each semiconductor. AlSb and AlN are seen to have different CNL energies from Fig. 7(a). Fig. 9 shows the local density of states for an atomic layer away from the interface calculated using the SX hybrid functional. The valence band offsets VBO can be read off from Fig. 9 as the difference of the intercept of the PDOS with the energy axis. The VBO values for the six interfaces ZnTe:GaN, ZnTe:AlN, ZnTe:ZnO, AlSb:GaN, AlSb:AlN and AlSb:ZnO are listed in Table 3. The deviation of this VBO value from the CNL difference (green) or the EA difference (blue), is plotted against the calculated supercell VBO on the horizontal axis in Fig 10. The VBO difference for the case of the CNL rule can be derived from eqn (2) using S=0, because the dielectric constants of ZnTe and AlSb as large, so that S is very small. We note that the green points lie closer to the zero deviation axis than the blue points. This shows that the data are closer to the CNL matching limit overall, although there is some error in the CNL points. The error could result from two factors, first that the test systems ZnO and ZeTe had shallow cation cores, and second, the effect of the dangling bonds at the interface as in Fig 8(b).

	Supercell calculation (eV)	VBO using EA rule (eV)	deviation from EA rule (eV)	VBO using CNL matching rule (eV)	Deviation from CNL rule (eV)
AlSb/GaN	1.8	1.7	-0.28	1.6	-0.11
AlSb/AlN	2.75	1.8	-0.42	2.6	-0.05
AlSb/ZnO	2.9	2.2	-0.17	2.8	-0.03
ZnTe/GaN	0.92	1.3	0.41	1.0	0.09
ZnTe/AlN	1.85	1.4	-0.24	2.0	0.08
ZnTe/Zno	1.75	1.8	0.03	2.2	0.26

Table 3. Comparison of the valence band offsets (VBOs) calculated by using the supercell DFT calculation using the SX functional, and those from the electron affinity (EA) rule and from the CNL energy matching rule, and the deviation of each model from the supercell calculation.

2D materials

Heterojunctions of the transition metal dichalcogenides (TMDs) and similar semiconductors have been studied for many applications, including the tunnel field effect transistor (TFET). The TFET is a transistor design with a particularly sharp turn-on characteristic or ‘steep slope’ needed for low power computation.[61] TFETs use the heterojunction between vertically stacked layers of different TMDs with a type II / III band alignment. The advantage is that the van der Waals bonding between the layers does not require the layers to be lattice matched, so that in principle a heterojunction without defects is possible. This differs from a typical III-V semiconductor heterojunction which often have mismatch defects which degrade their turn-on characteristic.

Many workers[61-63] have calculated the band offsets of stacked TMD heterojunctions within the electron affinity model. We have calculated the electron affinities, ionisation potentials, and charge neutrality levels for both bulk and monolayer versions in the SX functional[63] as in Fig.

11. Explicit supercell calculations for stacked heterojunctions found that the EA model did hold in this case[63].

It is also possible to make the lateral heterojunction where the layers of the two compounds are directly bonded to each other. Interestingly, reasonably abrupt junctions have been achieved between TMDs experimentally, even when not fully lattice matched.

These lateral heterojunctions, being fully bonded, are essentially the same as heterojunctions of 3D semiconductors. It has been tested whether they follow the CNL matching rule or the electron affinity rule by calculating the band offsets using supercell calculations. Generally, it is found that they do obey the CNL matching rule[63,64], as summarised in Fig. 12. It is not yet clear if there has been a good experimental test of this behaviour. Nevertheless, Fig. 12 indicates that 2D semiconductors present a good test of both the no charge transfer and screened limits for band offsets at heterojunctions.

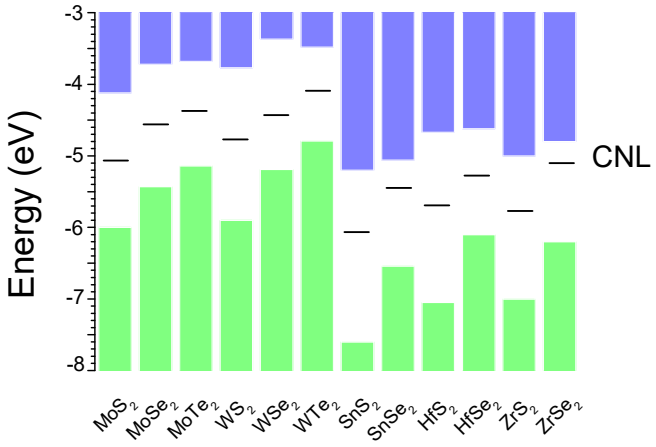

Fig. 11. Electron affinities, ionisation potentials and CNLs of various metal dichalcogenides calculated by the SX functional.

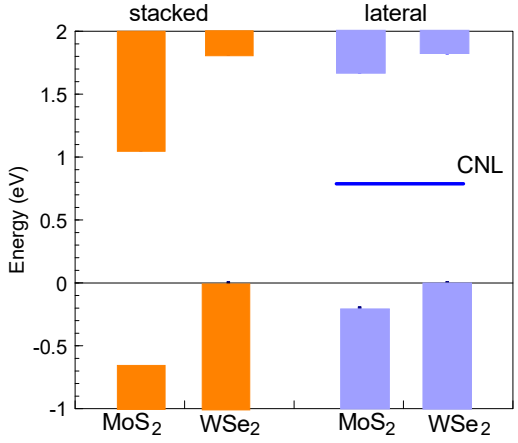

Fig. 12. Comparison of the band alignments for stacked and lateral junctions, calculated for supercells.

Discussion

Pinning limits for Schottky barriers vs. Semiconductor interfaces

The degree of pinning at its Schottky barriers for a particular semiconductor can be derived in experiment or modelling by evaluating S, the rate of change of Schottky barrier height with contact metal work function. On the other hand, and despite our results in Fig 10, why is the equivalent question of evaluating the degree of pinning at one of its semiconductor interfaces much more difficult?

Experimentally, there is no need to use lattice-matched metals on semiconductors to evaluate SBHs, so a wide range of data is available, including a very wide range of effective work function values[34]. In contrast, semiconductor band offsets need matched heterojunctions, otherwise defects form which pin E_f and so interfere with the band offset value.

Similarly, in DFT modelling, Schottky interfaces between badly matched metals and semiconductors can be made; any defects would just create states in the metal's continuum. This is not so for the case of semiconductors, badly chosen matching would cause electronic defects which would negate the model.

Related questions

The weak dependence of the CNL energy on the average of the electron affinity and ionisation potentials from Fig. 7 helps to explain a number of other diverse effects.

The first effect is the behaviour of interstitial hydrogen in semiconductors. Hydrogen can have two basic behaviours[39,66,67], (a) as a shallow donor, with its +1/0 and 0/ -1 levels lying at the CBM, (b) as a deep amphoteric defect with its +1/0 and 0/-1 levels deep in the gap, and usually showing a 'negative-U' property. In the tetrahedral semiconductors, van der Walle and Neugebauer[39] showed the remarkable property that interstitial hydrogen's +1/-1 level lay at an almost constant energy below the vacuum level for all these semiconductors, and including SiO_2 and water. This result implies that there is a constant reference energy for H, the vacuum level. A similar result but with more scatter is found to occur for interstitial hydrogen in oxides.[66]

Van de Walle and Neugebauer[39] explained this behavior of hydrogen as a breaking of a C-A bond (c=cation, a=anion), with H bonding to the C in the +1 state and H bonding to the A in the -1 state. The sites with a bonded hydrogen would have four bonds and so be passivated, leaving a cation dangling bond for the +1 state and an anion dangling bond for the -1 state. The overall result would be that the +1/-1 transition level would lie the average energy of the cation and anion DBs, which is similar to the CNL energy. Thus, this mechanism would argue for the +1/-1 state would be roughly the CNL energy, and not particularly related to the vacuum level. Only in the case of water should there be a relationship to the vacuum level via the electrochemical series. However, if, for a narrow set of semiconductors, the CNL energy actually varies little, as occurs in Fig 7, then the vacuum level could act as a reasonable reference energy.

The second effect is doping limits. It was found empirically that the maximum dopant concentration in a semiconductor corresponded to it being able to move its Fermi energy only within certain energy limits, on either the n- or p-type side.[68] Beyond that, the dopant makes compensated defect complexes which stop further movement of E_F. If these energies are within the band gap rather than in the bands, then that semiconductor cannot be doped for that polarity. An energetic analysis of this behaviour showed that the dopant becomes compensated by an

intrinsic defect of the opposite sign, and the doping limit then corresponds to an E_F where the compensating defect will form spontaneously. The defect have a zero formation energy at this E_f value[69]. Should these doping limit energies be constant with respect to a particular semiconductor's reference energy, such as its CNL, or should they be relatively independent of material and referred to the vacuum level? It turns out that it is difficult to differentiate between these two cases using the available data[40]. Fig. 7 provides some resolution to this question, because the CNL energy does not vary so much with the average of EA and IP, so both cases can hold at the same time. It will need better data, calculations, or a special materials system to differentiate between these two cases.

Conclusions

DFT supercell calculations are used to calculate the band offsets at semiconductor heterojunctions and if these follow two extreme limits, the electron affinity rule (no charge transfer) and the CNL matching rule (finite charge transfer). It is shown that traditional tests of these limits are not very strong because average band energies have a strong correlation with average bond lengths, so tests between lattice-matched heterojunctions are not a strong test. By using the case of a 1.41 lattice-mismatch, this provides a stronger test, which is found to support the CNL matching case.

The fact that in most 3D-bonded semiconductors that the CNL lies at a relatively constant energy below the vacuum level explains two other observations, that the +1/-1 energy level of the interstitial hydrogen should lie at a relatively constant energy, also that the doping limits lie at relatively constant energies below the vacuum level.

Acknowledgements

The authors acknowledge funding from EPSRC grant EP/P005152/1, EC grant No 711792 and the China Scholarship Council.

Conflict of Interest

The authors declare no conflict of interest.

References

1. Tung, R., T.; Physics and Chemistry of the Schottky Barrier Height, *App Phys Rev* **2014,** *1,* 011304
2. Wei, S. H.; Zunger, A.; Calculated Natural Band Offsets of all II-VI and III-V Semiconductors , *Appl. Phys. Lett.* **1998,** *7,2*2011
3. Harrison, W. A.; Elementary Theory of Heterojunctions, *J. Vac. Sci. Technol.* **1977,** *14*, 1016 -1020
4. Tersoff, J.; Theory of Semiconductor Heterojunctions – Role of Quantum Dipoles, *Phys. Rev. B* **1984,** *30*, 4874-4877
5. Tersoff, J.; Schottky Barrier Heights and the Continuum of Gap States, *Phys. Rev. Lett.* **1984,** *52,* 465-468
6. Harrison, W. A.; Tersoff, J.; Tight-binding Theory of Heterojunction Band Lineups and Interface Dipoles, *J. Vac. Sci. Technol. B* **1986,** 4, 1068 -1073
7. Baldereschi, A., Baroni, S., Resta, R.; Band Offsets in Lattice-matched Heterojunctions. *Phys. Rev. Lett.* **1988,** *61*, 734 -737
8. Hinuma, Y., Gruneis, A., Kresse, G., Oba, O.; Band Alignment of Semiconductors from Density Functional Theory and Many-body Perturbation Theory, *Phys. Rev. B* **2014,** *90*, 155406
9. Hinuma, Y., Kumagai, Y., Tanaka, I., Oba, F.; Band Alignment of Semiconductor using Dielectric Dependent Hybrid Functionals, *Phys. Rev. B* **2017,** *95,* 075302
10. Steiner, K., Chen, W., Pasquarello, A.; Band Offsets of Lattice-matched Semiconductor Heterojunctions through Hybrid Functional and G0W0, *Phys. Rev. B* **2014,** *89,* 205309
11. Robertson, J.; Band Offsets of Wide Band Gap Oxide and Implications for Future Electronic Devices, *J Vac Sci Technol B* **2000,** *18*, 2760-2769
12. Monch, W.; Role of Virtual Gap States and Defects in Metal-Semiconductor Contacts, *Phys. Rev. Lett*. **1987,** *58*, 1260 -1263
13. Tung, R., T.; Chemical Bonding and Fermi Level Pinning at Metal-Semiconductor Interfaces, *Phys. Rev. Lett*. **2000,** *84*, 6078
14. Wei, S., H.; Zunger, A.; Role of d Orbitals in Valence Band Offsets of Common Anion Semiconductors, *Phys. Rev. Lett.* **1987,** *59,* 144-147
15. Chen, W., Pasquarello, A.; Correspondence of Defect Energy Levels in Hybrid Functional Theory and Many-body Perturbation Theory, *Phys. Rev. B* **2013,** *88,* 115104
16. Chen, W., Miceli, G., Rignanese, G. M., Pasquarello, A.; Non-empirical Dielectric Dependent Hybrid Functional with Range Separation for Semiconductors and Insulators, *Phys. Rev. Mater*. **2018,** *2,* 073803
17. Hwang, J.; Wan, A., Kahn, A.; Energetics of Metal-organic Interfaces, new Experiments and Assessment of the Field, *Mater. Sci. Eng. R* **2009,** *64,* 1
18. Braun,S.; Salaneck, W. R.; Fahlmann, M.; Energy Level Alignment at Organic/Metal and Organic/Organic Interfaces, *Adv Mater* **2009,** *21,* 1450-1472
19. Duhm, S.; Heimel, G.; Salzmann, I,; Glowatzki, H.; Johnson, R L.; Vollmer, A.; Rabe, J P.; Koch, N.; Orientation-dependent Ionization Energies and Interface Diploes in Ordered Molecular Assemblies, Nature Mater **2008,** *7,* 326
20. Li, Y.; Li. P.; Lu, Z. H.; Mapping Energy Levels for Organic Heterojunctions, Adv Mater **2017,** *29,* 1700414
21. Clark, S. J., et al; First principle methods using CASTEP, *Zeitschrift Krystallogr*. ***2005,*** 220, 567-571
22. Grimme, S.; Semi-empirical GGA type Density Functional with Long-range Dispersion Correction, J. Comput. Chem. **2006,** *27*, 1787
23. Heyd, J., Scuseria, G., E., Ernzerhof, M.; Hybrid Functional Based on a Screened Coulomb Potential, *J. Chem. Phys.* **2006,** *124*, 219906
24. Clark, S. J., Robertson, J., Screened Exchange Density Functional Applied to Solids, *Phys. Rev. B* **2010**, *82,* 085208

25. Lany, S., Zunger, A.; Polaronic Hole Localisation and Multiple Hole Binding in Wide-gap Semiconductors, *Phys. Rev. B* **2009,** *80,* 085202
26. Komsa,H. P., Broqvist, P., Pasquarello, A.; Alignment of Defect levels and Band Edges through Hybrid Functionals; Effect of Screening in the Exchange Term, *Phys. Rev. B* **2010,** *81,* 205118
27. Marques, M. A. L., Vidal, J., Oliveira, M. J. T., Reining, L., Botti, S.; Density Based Mixing Parameter for Hybrid Functionals, *Phys. Rev. B* **2011,** *83,* 035119
28. Brillson, L., 'Surfaces and Interfaces of Electronic Materials', (Wiley-VCH, 2010) p549.
29. Hosono, H.; Exploring Electro-active Functionality of Transparent Oxide Materials, *Jpn. J. Appl. Phys*. **2013,** *52,* 090001
30. Klein, A.; Interface Properties of Dielectric Oxides, J. Amer. Ceram Soc **2016,** *99,* 369
31. Li, S.; et al, Intrinsic Energy Band Alignment of Functional Oxides, *Phys. Stat. Solidi. RRL* **2014,** *8,* 571 -578
32. Iwai, H.; Past, Present and Future of High K/Metal Gate Technologies, *ECS Trans* **2017,** *80,* 3-16
33. Greiner, M. T., Helander, M. G., Tang, W. M.; Wang, Z. B., Qiu, J., Lu, Z. B.; Universal Energy-level Alignment of Molecules on Metal Oxides, *Nature Mater*. **2011,** *11,* 76
34. Robertson, J.; Band Offsets, Schottky Barrier Heights, and their Effect on Electronic Devices, *J Vac Sci Technol A* **2013,** *31* ,050821
35. Oba, F., Togo, A., Tanaka, I., Paier, J., Kresse, G.; Defect Energetics in ZnO Hybrid Functional study, Phys. Rev. B **2008** *77,* 245202
36. Stevanovic, V., Lany, S., Ginley, D. S., Tumas, W., Zunger, A., Assessing Capability of Semiconductors to Split Water using Ionization Potentials and Electron Affinities, *Phys Chem Chem Phys* **2014,** *16,* 3706
37. Li, Y. H., Walsh, A., Chen, S. Y., Yin, W., Yang, J. H., Li, J., B., DaSilva, J., B. H. Gong, X. G., Wei, S. H.; Revised Ab-initio Natural Band Offsets of Group IV, II-VI and III-V Semiconductors, *Appl. Phys. Lett*. **2009,** *94*, 212109
38. Guo, Y. Robertson, J., Clark, S. J.; Effect of Screening Length in the Non-local Screened Exchange Functional, *J. Phys. Conden. Mater*. **2015,** *27,* 025501
39. van der Walle, C. G., Neugebauer, J.; *Nature* **2003,** *423,* 626
40. Robertson, J., Clark, S. J., Limits to Doping in Oxides, *Phys. Rev. B* **2011,** *83,* 075205
41. Scanlon, D.O., Watson, G. W., Undoped n-type Cu_2O, Fact or Fiction, *J. Phys. Chem. Lett*. **2010,** *1,* 2582
42. Gillen, R., Robertson, J.; Band Structure Calculations of $CuAlO_2$, $CuGaO_2$, $CuInO_2$ and $CrCuO_2$ by Screened Exchange, *Phys. Rev. B* **2011,** *84,* 035125
43. Nie, X., Wei, S.H., Zhang, S. B.; Bipolar Doping and Band-gap Anomalies in Delafossite Transparent Conductive Oxides, *Phys. Rev. Lett*. **2002,** *88,* 066405
44. Scanlon, D. O., Watson, G. W.; Conductivity Limits in $CuAlO_2$ from Screened Hybrid Density Functional Theory, *J Phys. Chem. Lett*. **2010,** *1,* 3195
45. Robertson, J.; *Rep. Prog. Phys*. **2006,** *69,* 327
46. Gillen,R., Clark, S. J., Robertson, J.; Nature of the Band Gap in Lanthanide Oxides, *Phys. Rev. B* **2013,** *87,* 125116
47. Clark,S. J., Robertson, J.; Band gap and Schottky Barrier Heights of Multiferroic $BiFeO_3$, *Appl. Phys. Lett*. **2008,** *90,* 132903
48. Gillen, R., Robertson, J.; Accurate Screened Exchange Band Structures for Transition Metal Monoxides MnO, FeO, CoO and NiO, *J. Phys. Conden. Mater*. **2013,** *25* ,165520
49. Monch, W.; Empirical Tight-binding Calculation of the Branch Point energy of the Continuum of Interface-induced Gap States, *J. Appl. Phys*. **1996,** *80*, 5076-5082
50. Robertson, J., Falabretti, B.; Band Offsets of High K Oxides on Semiconductors, *J. Appl. Phys*. **2006,** *100,* 014111
51. Peacock, P. W., Robertson, J.; Band Offsets and Schottky Barrier Heights of High Dielectric Constant Oxides, *J. Appl. Phys*. **2002,** *92,* 4712

52. Hoffling, B., Schleife, A., Rodl, A., Bechstedt, F.; Band Discontinuities at Si-TCO Interfaces from Quasi-particle Calculations, *Phys. Rev. B*, **2012,** *85,* 035305
53. Schliefe, A., Fuchs, F., Rodl, C., Furthmuller, C., Bechstedt, F.; Band Lineup between Silicon and Transparent Conducting Oxides, *Appl. Phys. Lett.* **2009,** *94* 012104
54. Cardona, M., Christensen, N. E.; Acoustic Deformation Potentials and Heterostructures Band Offsets, *Phys. Rev. B* 1**987,** *35,* 6182
55. Chang, Y., C.; Complex Band Structures of Zincblende Materials, *Phys. Rev. B* **1982,** *25,* 605
56. Dederichs, P. H., Mavropoulos, P., Wunnicke, O., Papnikolaou, N., Bellini, V., Zeller, R., Drchal, V., Kudrnovsky, V., Importance of Complex Band Structure and Resonant States for Tunnelling, *J. Mag. Mag. Mater*. **2002,** *240*, 108- 113
57. Demkov, A. A., Fonseca,L. R. C., Verret, E., Tomfohr, J., Sankey, O. F., Complex Band Structure and Band Alignment Problem at Si-High-K Dielectric Interface, *Phys. Rev. B* **2005,** *71,* 195306
58. Cowley, A. M., Sze, S. M.; Surface States and Barrier Height of Metal-Semiconductor Systems, *J. Appl. Phys.* **1965,** *36,* 3212-3220
59. Yu, E. T., McCaldin, J. O., McGill,T. C.; Band Offsets in Semiconductor Heterojunctions, *Solid State Physics*, **1992,** *46* 1, (Academic Press),
60. Katnani, A. T., Margaritondo, G.; Microscopic Study of Semiconductor Heterojunctions, *Phys. Rev. B* **1983,** *28,* 1944-1956
61. Gong, C., Zhang, H., Wang, W., Colombo, L., Wallace, R. M., Cho, K. J.; Band Alignment of two-Dimensional Transition Metal Dichalcogenides, Application to Tunnel Field Effect Transistors, *Appl. Phys. Lett.* **2013,** *103,* 053513
62. Kang, J.,Tongay, S., Zhou, J., Li, J., Wu, J.; Band Offsets and Heterostructures of Two-dimensional Semiconductors, *Appl. Phys. Lett.* **2013,** *102,* 012111
63. Guo, Y., Robertson, J.; Band Engineering in Transition metal Dichalcogenides, Stacked vs Lateral Heterostructures, *Appl. Phys. Lett* **2016,** *108,* 233104
64. Guo, Y., Liu, D., Robertson, J.; 3D Behaviour of Schottky Barriers of 2D Transition Metal Dichalcogenides, *ACS Appl Mater Interfaces* **2016,** *7,* 25709
65. Greiner, M. T., Chai, L., Helander, M. G., Tang, W. M., Lu, Z. H., *Adv. Funct. Mater* **2012**, *22*, 4557-4568
66. Li, H., Robertson, J.; Hydrogen in Wide band-gap Oxides, *J. Appl. Phys*. **2014,** *115,* 203708
67. Kilic, C., Zunger, A.; N-type Doping of Oxides by Hydrogen, *Appl. Phys. Lett*. **2002,** *81,* 73-75
68. Walukiewicz, W.; Intrinsic Limitations to Doping of Wide-gap Semiconductors, *Physica* **2001,** *302-303,* 123 -134
69. Zhang, S. B., Wei, S., H., Zunger, A.; Phenomenological Model for Systematization and Prediction of Doping Limits in II-VI and III-V Compounds, *J. Appl. Phys*. **1998**,*83,* 3192-3196

.